

Contributions to the homogeneous plastic flow of *in situ* metallic glass matrix composites

X. L. Fu

Singapore-MIT Alliance, National University of Singapore, Singapore 117576, Singapore

Y. Li

Singapore-MIT Alliance and Department of Materials Science and Engineering, Faculty of Engineering, Engineering Drive 1, National University of Singapore, Singapore 117576, Singapore

C. A. Schuh^{a)}

Department of Materials Science and Engineering, Massachusetts Institute of Technology, Cambridge, Massachusetts 02139

(Received 28 July 2005; accepted 31 October 2005; published online 5 December 2005)

The homogeneous deformation of Zr-based bulk metallic glass composites is studied near the glass transition temperature, at various levels of reinforcement volume fraction. Through examination of the constitutive response, it is seen that the presence of *in situ* reinforcements increases the flow resistance of the glass dramatically. This strengthening effect is shown to arise from two separate contributions: load transfer from the amorphous matrix to the reinforcements, and changes to the glass composition and structure upon *in situ* precipitation of reinforcements. © 2005 American Institute of Physics. [DOI: 10.1063/1.2140477]

The high-temperature rheology of supercooled liquid metals and metallic glasses has been of fundamental interest for decades,¹⁻³ and the recent development of bulk glass-forming alloy compositions has precipitated more detailed studies and greater understanding of such high-temperature deformation.⁴⁻¹⁰ The superplastic-like flow of metallic glasses is considered a technological advantage for forming of complex shapes, but at the same time, macroscopic brittleness at low temperatures has posed a significant problem for technological insertion. A number of efforts are currently underway to improve the ductility of metallic glasses, most notably the development of second-phase reinforced bulk metallic glass matrix composites (BMGMCs).¹¹⁻¹⁶ While it has now been demonstrated by several authors that second phase reinforcements can improve the room-temperature mechanical properties of metallic glasses,^{11,13,17-19} it remains unclear how such reinforcements impact their high-temperature homogeneous flow. In particular, the mechanisms by which reinforcements affect the rheology and superplastic deformation of metallic glasses have not been studied, and our purpose here is to identify these mechanisms for the first time.

Following the developments of several groups working in this area,^{11,12,20,21} we have used an *in situ* approach to form BMGMCs directly from the melt in the Zr-Cu-Al system. Rods 5 mm in diameter were prepared from four different alloy compositions, by arc melting high purity metals and subsequently casting into copper molds under an argon atmosphere. The compositions studied were of the form $Zr_{49}Cu_{51-x}Al_x$ with $x=6, 8, 10,$ and 12 at. %, and the microstructures of these alloys are depicted in Fig. 1. Here we observe that the gradual substitution of Al for Cu promotes phase separation during processing; x-ray diffraction revealed only two phases in these alloys, an amorphous matrix and reinforcements of τ_3 phase, $Zr_{51}Al_{21}Cu_{28}$.²¹ The second

phase generally appears as isolated dendrites with shapes reflecting an underlying crystal symmetry, although at the highest aluminum concentration [Fig. 1(d)] some of the dendrites exhibit a more irregular rosette morphology.

As Fig. 1 illustrates, higher aluminum concentrations are found to increase the volume fraction of second phase dendrites in these BMGMCs, and in the remainder of this letter we will label each material with its respective reinforcement volume fraction (called f), as determined by image analysis. However, the composition changes in these alloys also affected the chemistry and/or structure of the amorphous matrix, as evidenced by a slight increase in the glass transition temperature measured by differential scanning calorimetry (DSC). Figure 2 shows the DSC curves obtained for these alloys, with the onset glass transition temperature, T_g , denoted by arrows; the inset graph plots T_g as a function of the reinforcement volume fraction to clarify the effect.

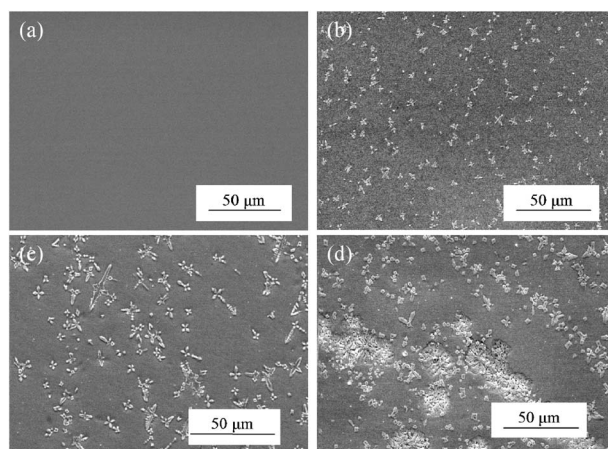


FIG. 1. Scanning electron micrographs of (a) the Zr-based bulk metallic glass and the *in situ* composites used in this work, containing (b) 7%, (c) 15%, and (d) 20% of the dendritic second phase. These alloys have compositions $Zr_{49}Cu_{51-x}Al_x$ with $x=6, 8, 10,$ and 12 at. %, for the four structures, respectively.

^{a)} Author to whom correspondence should be addressed; electronic mail: schuh@mit.edu

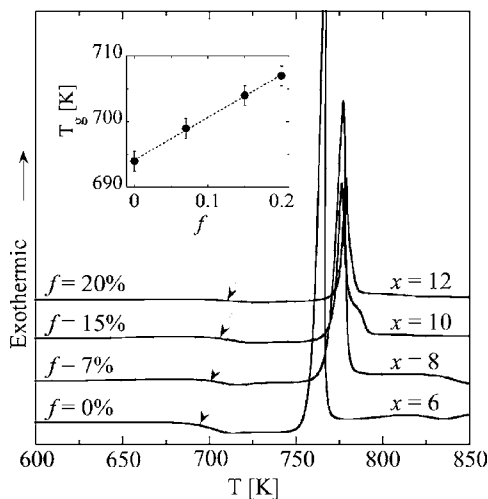


FIG. 2. Differential scanning calorimetry data (scan rate = 20 K min⁻¹) for the metallic glass alloy (Zr₄₉Cu_{51-x}Al_x with x = 6) and *in situ* composites with different aluminum contents (x = 8, 10, 12) and volume fractions of reinforcement (f); the onset glass transition temperature (T_g) is denoted by an arrow in each case. In the inset T_g is plotted as a function of f, where it is seen that the glass transition in the composite specimens is shifted from that in the monolithic glass.

The high-temperature mechanical properties of the four alloys were investigated through conventional hot compression tests at a temperature of $T = 693$ K, close to the glass transition of the unreinforced ($f = 0$) glass composition. The test specimens were right cylinders of 10 mm length and about 5 mm diameter, machined from the cast rods and mechanically polished on all surfaces to 0.05 μm prior to testing. Constant displacement-rate tests were performed and strain was monitored with conventional extensometry and a linear voltage-displacement transducer; no specimen was subjected to more than a single deformation rate. For the sake of brevity we do not present the stress-strain curves obtained from these tests, but the results were in line with expectations for homogeneous flow of metallic glasses: at higher rates there was a stress overshoot followed by steady-state flow, while at lower rates the overshoot was absent and flow stabilized quickly to a steady-state.

Figure 3 plots the combinations of true stress, σ , and true strain rate, $\dot{\epsilon}$, found in steady-state for each of the four alloys. In the double-logarithmic format of Fig. 3, the slope of the data reflects the strain rate sensitivity, which is highest at lower rates and decreases quickly as the strain rate rises. This behavior is expected for homogeneous flow of amorphous metals, and has been explained using models based on free-volume evolution²² and local shear transitions.²³ Both of these types of models have the same basic form, and here we will adapt the shear-transition model of Ref. 23 to uniaxial loading, for which the steady-state strain rate should obey the following phenomenology:

$$\dot{\epsilon} = \dot{\epsilon}_0 \cdot \sinh\left(\frac{\sigma}{\sqrt{3}} \frac{\gamma_0 V}{kT}\right). \quad (1)$$

Here $\dot{\epsilon}_0$ is a temperature-dependent constant, $\gamma_0 \approx 0.125$ is the characteristic shear associated with the atomic-scale rearrangements that accommodate strain, V is the characteristic volume associated with such rearrangements, and k is Boltzmann's constant. Equation (1) is directly applicable for an unreinforced metallic glass ($f = 0$), and in the present case it

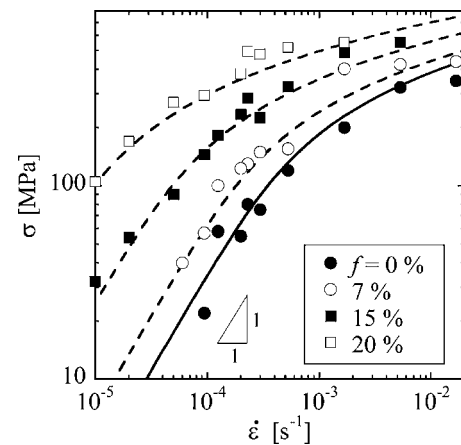


FIG. 3. Homogeneous flow data at $T = 693$ K for the Zr-based metallic glass and *in situ* composites with various reinforcement volume fractions, f . Steady-state flow stress is presented as a function of applied strain rate on double-logarithmic scales, and the lines are best-fits of Eq. (1).

can be credibly fitted to the experimental data; this is illustrated by the solid trendline in Fig. 3, which uses as fitting parameters $\dot{\epsilon}_0 = 2.5 \times 10^{-4} \text{ Pa}^{-1} \text{ s}^{-1}$ and $V = 1.5 \times 10^{-27} \text{ m}^3$. The latter volume is large enough to contain several dozen atoms, which is in line with the understanding of local shear events in metallic glass deformation.²³

In the case of the reinforced BMGMCs, we expect that the deformation is likely carried solely by the amorphous matrix phase, which is near T_g and soft compared with the intermetallic reinforcements. Accordingly, the same basic flow mechanisms that operate in the unreinforced glass are expected to occur in the matrix of the composites, and, in principle, the value of V should not change appreciably as reinforcements are added. Therefore, with only a single adjustable parameter ($\dot{\epsilon}_0$), it should be possible to fit the flow data of the composites. This expectation is borne out by the dashed lines in Fig. 3, which plot the fitted form of Eq. (1) using the same characteristic volume V obtained earlier for the unreinforced glass. The resulting fitted values of $\dot{\epsilon}_0$ are normalized to that obtained at $f = 0$, and collected in Fig. 4 as a function of the reinforcement volume fraction.

With satisfactory fits of Eq. (1) to our steady-state flow data, we may now consider the mechanisms by which $\dot{\epsilon}_0$ is changed as the reinforcement volume fraction is increased. For this purpose we will limit our attention to the Newtonian flow regime, which is the low-stress regime characterized by a strain rate sensitivity of unity in Fig. 3. Although the experimental data do not all reach the Newtonian regime, extrapolation is straightforward using Eq. (1), which reduces in the low stress limit as

$$\dot{\epsilon} \propto \dot{\epsilon}_0 \cdot \sigma \quad (2)$$

and we see that $\dot{\epsilon}_0$ is inversely proportional to the Newtonian viscosity. The reason for focusing upon Newtonian flow pertains to the mechanics of time-dependent deformation in composites; closed-form models are available to account for the effects of load sharing between matrix and reinforcement in the Newtonian case. In this work we will use the model of Lee and Mear,²⁴ which is a continuum treatment that can describe the deformation of a composite when load is shared between the matrix and reinforcement due to strain mismatch. For roughly equiaxed reinforcements such as we have here, their result can be written

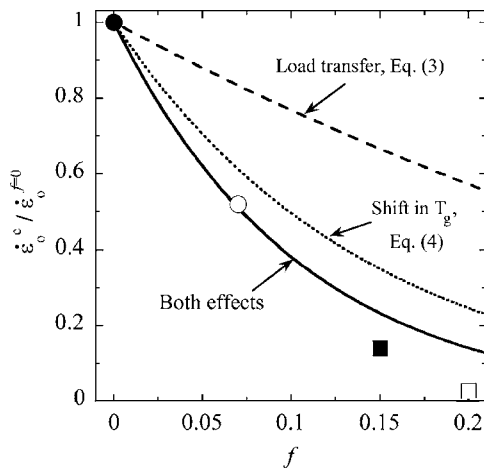


FIG. 4. Newtonian flow rates at $T=693$ K for the *in situ* composite specimens, normalized by that of the unreinforced glass that nominally comprises the matrix phase; symbols are the same as those in Fig. 3. Points are the values extracted from the experiments through best fitting with Eq. (1), while the lines denote theoretical predictions of Eqs. (3) and (4).

$$\dot{\epsilon}_0^c = \dot{\epsilon}_0^m (1 - f)^{5/2}, \quad (3)$$

where the superscripts “c” and “m” denote composite and matrix properties, respectively. The predictions of Eq. (3) are plotted in Fig. 4 (dashed line); when compared with the experimental data it is clear that typical composite strengthening through load transfer is insufficient to explain the strength of these BMGMCs at any volume fraction.

Since load sharing is apparently not solely responsible for the reduced deformation rates of the present composites, we seek a second strengthening mechanism that arises upon adding crystalline reinforcements. As noted earlier with reference to Fig. 2, the *in situ* processing technique used to synthesize these BMGMCs also somewhat affects the composition and/or structure of the glassy matrix. Higher aluminum concentrations lead to higher values of f , and at the same time raise T_g (inset to Fig. 2). Because their glass transitions are higher than that of the unreinforced glass, the BMGMCs were actually tested at somewhat lower homologous temperatures (T/T_g); the glassy matrix has been strengthened in these composites, as reflected in a higher T_g .

In order to estimate the degree of strengthening in the glassy matrix of these BMGMCs, we note that $\dot{\epsilon}_0$ contains a thermal activation term

$$\dot{\epsilon}_0 \propto \exp\left(-\frac{Q}{kT}\right), \quad (4)$$

where Q is the activation energy for viscous flow, and is of the order $40\text{--}100kT_g$ for a typical metallic glass. In the current scenario, as the glass transition increases from one composite to the next, the activation energy for flow should increase proportionally, and the deformation rate would decrease according to Eq. (4). We estimate this effect by taking $Q \approx 75kT_g$ (calculated for our Zr-based glass using the model of Argon,²³) and using the linear relationship between T_g and f observed in the experimental data of Fig. 2.

The predictions of Eq. (4) can be compared with the experimental data, as shown by the dotted line in Fig. 4. As

before, we find that this strengthening mechanism alone cannot reproduce the trend exhibited by the experimental data. However, when the effects of both matrix hardening and composite load sharing are combined (solid line in Fig. 4), we find the agreement with the experimental data is reasonable.

Based on this discussion, we conclude that the incorporation of *in situ* reinforcements leads to strengthening of metallic glass in two complementary ways as regards homogeneous flow: (1) the deforming matrix phase sheds load to the rigid reinforcements, and (2) the matrix is hardened by virtue of the composition shift associated with *in situ* composite processing. It is somewhat surprising to observe that the hardening effect within the glass matrix is actually more significant than is the composite load-sharing effect (Fig. 4), especially given the relatively subtle shift (~ 12 K) in the glass transition temperature (Fig. 2). Of course, the relative importance of these two effects may be different from one family of BMGMCs to the next, and it is conceivable that the two mechanisms may compete with one another if the system chemistry is such that the matrix is weakened (T_g is lowered) upon precipitation of *in situ* reinforcements. In any case, viscous shape forming operations and future studies of rheology in BMGMCs should be performed in cognizance of both strengthening mechanisms.

This work was supported by the Singapore-MIT Alliance, as well as the US Army Research Office under Contract No. DAAD19-03-1-0235; the views expressed in this work are not endorsed by the sponsors. The authors gratefully recognize the experimental involvement of Dr. M. L. Lee and Mr. D. Wang (National University of Singapore) as well as A. J. Detor (MIT).

¹D. E. Polk and D. Turnbull, *Acta Metall.* **20**, 493 (1972).

²J. Megusar, A. S. Argon, and N. J. Grant, *Mater. Sci. Eng.* **38**, 63 (1979).

³A. I. Taub and F. Spaepen, *Acta Metall.* **28**, 1781 (1980).

⁴R. Busch, E. Bakke, and W. L. Johnson, *Acta Mater.* **46**, 4725 (1998).

⁵Y. Kawamura, T. Shibata, A. Inoue, and T. Masumoto, *Appl. Phys. Lett.* **69**, 1208 (1996).

⁶T. G. Nieh, J. Wadsworth, C. T. Liu, T. Ohkubo, and Y. Hirotsu, *Acta Mater.* **49**, 2887 (2001).

⁷M. D. Demetriou and W. L. Johnson, *J. Appl. Phys.* **95**, 2857 (2004).

⁸J. M. Pelletier, B. Van de Moortele, and I. R. Lu, *Mater. Sci. Eng., A* **336**, 190 (2002).

⁹C. A. Schuh, A. C. Lund, and T. G. Nieh, *Acta Mater.* **52**, 5879 (2004).

¹⁰M. D. Demetriou and W. L. Johnson, *Acta Mater.* **52**, 3403 (2004).

¹¹C. C. Hays, C. P. Kim, and W. L. Johnson, *Phys. Rev. Lett.* **84**, 2901 (2000).

¹²H. Tan, Y. Zhang, and Y. Li, *Intermetallics* **10**, 1203 (2002).

¹³D. H. Bae, M. H. Lee, D. H. Kim, and D. J. Sordelet, *Appl. Phys. Lett.* **83**, 2312 (2003).

¹⁴C. Fan, R. T. Ott, and T. C. Hufnagel, *Appl. Phys. Lett.* **81**, 1020 (2002).

¹⁵H. Choi-Yim and W. L. Johnson, *Appl. Phys. Lett.* **71**, 3808 (1997).

¹⁶U. Kuhn, J. Eckert, N. Mattern, and L. Schultz, *Appl. Phys. Lett.* **80**, 2478 (2002).

¹⁷F. Szuets, C. P. Kim, and W. L. Johnson, *Acta Mater.* **49**, 1507 (2001).

¹⁸M. L. Lee, Y. Li, and C. A. Schuh, *Acta Mater.* **52**, 4121 (2004).

¹⁹D. V. Louzguine, H. Kato, and A. Inoue, *Appl. Phys. Lett.* **84**, 1088 (2004).

²⁰G. He, W. Loser, J. Eckert, and L. Schultz, *J. Mater. Res.* **17**, 3015 (2002).

²¹D. Wang, H. Tan, and Y. Li, *Acta Mater.* **53**, 2969 (2005).

²²F. Spaepen, *Acta Metall.* **25**, 407 (1977).

²³A. S. Argon, *Acta Metall.* **27**, 47 (1979).

²⁴B. J. Lee and M. E. Mear, *J. Mech. Phys. Solids* **39**, 627 (1991).